

A Bioinformatics-Based Screening and Analysis of Key Genes in Hepatocellular Carcinoma

Yanfei Wei

Department of Physiology, Guangxi University of Chinese Medicine, Nanning, Guangxi, China, 530200

Shengshan Wang

Department of Physiology, Guangxi University of Chinese Medicine, Nanning, Guangxi, China, 530200

Wanjun Chen

Department of Physiology, Guangxi University of Chinese Medicine, Nanning, Guangxi, China, 530200

Yuning Lin

Department of Physiology, Guangxi University of Chinese Medicine, Nanning, Guangxi, China, 530200

Qi Zhang

Department of Physiology, Guangxi University of Chinese Medicine, Nanning, Guangxi, China, 530200

Delun Huang (✉ huangdelun0621@foxmail.com)

GuangXi University of Chinese Medicine <https://orcid.org/0000-0002-7449-0386>

Research

Keywords: hepatocellular carcinoma, bioinformatics, Key gene

Posted Date: December 22nd, 2020

DOI: <https://doi.org/10.21203/rs.3.rs-131655/v1>

License:  This work is licensed under a Creative Commons Attribution 4.0 International License.

[Read Full License](#)

A Bioinformatics-Based Screening and Analysis of Key Genes in Hepatocellular Carcinoma

YanFei Wei^{*}, ShengshanWang^{*}, Wanjun Chen, Yuning Lin, Qi Zhang, Delun Huang[#]

Department of Physiology, Guangxi University of Chinese Medicine, Nanning, Guangxi, China, 530200

^{*#}the authors contributed equally to this work.

Keywords: hepatocellular carcinoma; bioinformatics; Key gene

Address correspondence:

Delun Huang, Ph.D

Department of Physiology, Guangxi University of Chinese Medicine, Nanning, Guangxi 530001, China

Phone: 0771-4733794

Email: huangdelun0621@foxmail.com

1 **Abstract**

2 Hepatocellular carcinoma (HCC) is considered as the leading killer disease in the world. So
3 far most of the diagnosis of HCC is mainly established on imaging and biopsy. As sequencing
4 technology is developing quite fast, and it has already been widely applied in the medical area,
5 such as cancer diagnosis. In this article, GSE121248, GSE76427 and GSE60502 datasets were
6 chosen to analyze and screen key genes which could affect the development of liver cancer
7 through the bioinformatics method. The results showed up regulated genes mainly reside in
8 cell division, nucleus, protein binding pathway, and down regulated genes are mostly located
9 in the Oxidation-reduction process, Extracellular region, Heme binding, Metabolic pathway.
10 Secondly, hub gene analysis indicated there were twelve critical hub genes found: RFC4,
11 RACGAP1, CCNB2, CDC20, UBE2C, PTTG1, AURKA, PRC1, NCAPG, CDKN3, TOP2A,
12 KIF20A, AURKA and CDKN3. By applying bioinformatic measures, the genes associated
13 with hepatocellular carcinoma can be efficiently analyzed, that would provide invaluable
14 information for translational studies.

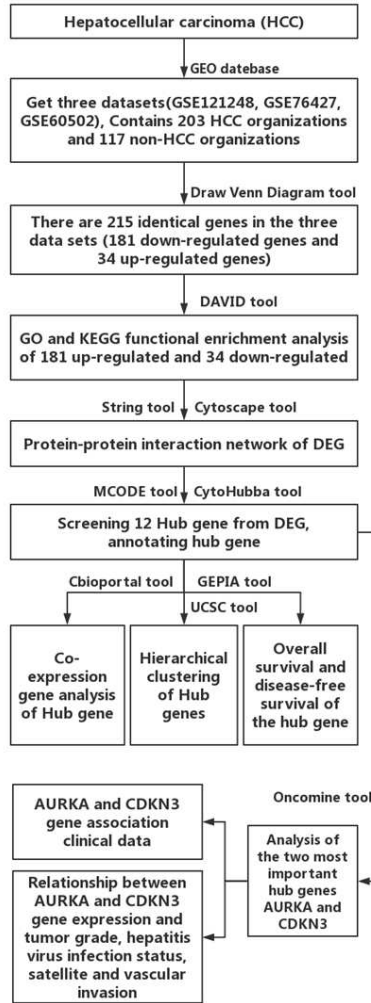
15

16 **Introduction**

17 Hepatocellular carcinoma (HCC) is the second leading cause of cancer-related deaths in the
18 world[1]. HCC is characterized by high mortality rates, high metastasis and high
19 invasiveness[2]. It is generally believed that the occurrence of HCC is associated with viral
20 infection (hepatitis C virus, hepatitis B virus), long-term alcohol consumption, Aflatoxin

21 infection, water contamination, nitrous acid substances, primary biliary cirrhosis and
22 non-alcoholic fatty liver, etc[3]. The treatment of early HCC mainly includes surgical
23 resection, liver transplantation, percutaneous radiofrequency ablation, and probably more
24 than 50% of patients have a five-year survival rate. Because the pathogenesis of HCC
25 involves multiple signaling pathways, and the molecular mechanisms of malignant
26 progression are unclear. Almost 80% of advanced-stage liver cancer patients have mainly
27 received radiotherapy and chemotherapy treatment. Therefore, identifying effective early
28 tumor diagnostic markers and targeted therapeutic targets is of great clinical significance [4].

29 The development of high-throughput gene chip and sequencing technology has helped
30 rapid the study of the gene expression profile of liver cancer, facilitating the discovery of gene
31 and gene expression changes of liver cancer tissues and cells subjected to specific conditions.
32 Due to the low reliability of positive results from a single microarray data analysis, in this
33 study, we analyzed three microarray datasets from the GEO database, each of them includes
34 HCC samples and non-tumor containing liver tissue samples. With the aid of GEO2R,
35 differential expressed genes (DEG) between HCC and normal samples were analyzed.
36 Applying several bioinformatics tools such as DAVID and String, the DEG's biological
37 functions, involved signaling pathways and interactions were worked out. Finally, 12 key
38 genes were selected to be candidate biomarkers for HCC. This study provides a theoretical
39 basis for the clinical screening of molecular markers and drug targets for the development and
40 progression of hepatocellular carcinoma (Fig.1).



41

42 **Fig. 1** The schematic of this study is intended to describe bioinformatics screening and analysis of key
 43 genes for HCC.

44 **1. Methods and materials**

45 **1.1 Obtaining Microarray Data** The National Center for Biotechnology Information's
 46 (NCBI) Gene Expression Omnibus (GEO, <https://www.ncbi.nlm.nih.gov/geo/>) is the largest
 47 public repository of high-throughput gene expression data[5]. To expand the sample size and
 48 improve the reliability of screening, three datasets of Homo tissue samples with both hepatic
 49 carcinoma and normal hepatic tissues included were selected. In our case, GSE121248[6],
 50 GSE76427[7] and GSE60502[8] datasets were screened out from the GEO database platform
 51 GPL570 ([HG-U133_Plus_2], Affymetrix Human Genome U133 Plus 2.0 Array), PL10558

52 (Illumina HumanHT-12 V4.0 expression bead chip) and GPL96 ([HG-U133A] Affymetrix
53 Human Genome U133A Array) respectively. GSE121248 contained 70 HCC samples and 37
54 adjacent non-tumor hepatic tissue samples, GSE76427 contained 115 HCC samples and 52
55 adjacent non-tumor hepatic tissue samples, while GSE60502 contained 18 HCC samples and
56 18 adjacent non-tumor hepatic tissue samples.

57 **1.2 Identification of DEG** The GEO2R (<http://www.ncbi.nlm.nih.gov/geo/geo2r/>) is an
58 R-based web application that enables to analyze GEO data between HCC samples and
59 non-cancer samples. The blank genome in each data set was removed, and genes with shared
60 IDs were also eliminated. A value of $|\logFC|$ (fold change) >1 and $P\text{-value}<0.05$ was taken to
61 be statistically significant. The Draw Venn Diagram
62 (<http://bioinformatics.psb.ugent.be/webtools/Venn/>) tool was then used to select upregulated
63 and downregulated genes common to all three datasets.

64 **1.3 GO and KEGG pathway enrichment analysis of DEG** DAVID
65 (<https://david.ncifcrf.gov/>) (version 6.8)[9] is a web-based online bioinformatics resource
66 which serves mainly to functionally interpret a large number of genes and protein. The
67 standard annotations for GO[10] biological functions include Biological Processes (BP),
68 Molecular Functions (MF) and Cellular Components (CC). KEGG[11] is a database resource
69 used particularly for genome sequencing and other high-throughput, large-scale molecular
70 information processing. Combining both GO and KEGG functions of the DAVID online tool,
71 DEG were analyzed with $p<0.05$ taken to be statistically significant.

72 **1.4 Protein-Protein Interaction (PPI) Network Analysis** The String (<https://string-db.org/>)

73 (version 11.0) [12] database is a database that searches for interactions between known
74 proteins and predicted proteins. In this experiment, multiple protein input forms were selected
75 and DEG data were imported, with Homo sapiens selected as the organism form. Setting
76 parameters: medium confidence=0.4, and default other parameters. Default all parameters,
77 then export the PPI data in TSV format. Cytoscape (version 3.7.1)[13] is a standard
78 application for bio-network analysis and visualization. The TSV text saved by String was
79 imported into cytoscape to create a PPI visualization network diagram. Using the MCODE
80 (version 1.5.1)[14] plugin in the Cytoscape database, setting parameters: k-core=2, Node
81 score cutoff=0.2, degree cutoff=2, and default other parameters. key genes of the PPI network
82 were filtered, and the closest set of key genes was selected. To increase the sensitivity and
83 specificity, we use MCC to discover featured nodes, We selected the Maximal Clique
84 Centrality algorithm (MCC) of the cytohubba plugin [15] in the Cytoscape tool to screen the
85 top Hub genes.

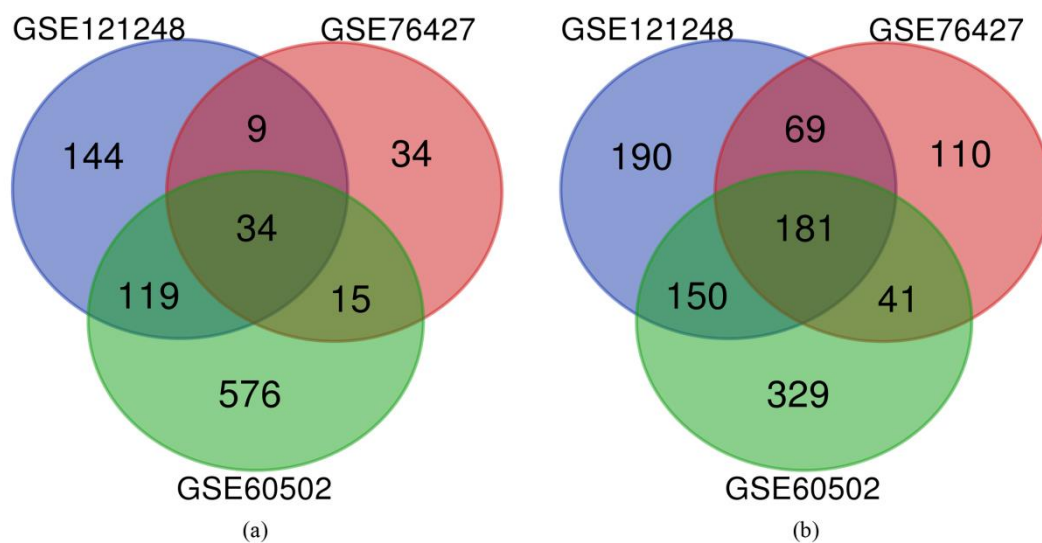
86 **1.5 Hub gene selection and analysis** cBioPortal for Cancer Genomics
87 (<http://cbioportal.org>)[16] is a web resource for exploring, visualizing, and analyzing
88 multidimensional cancer genomics data. This platform was used to analyze the 12 selected
89 key genes and co-expressed gene networks. The Gene Expression Profiling Interactive
90 Analysis (GEPIA) online database (<http://gepia.cancer-pku.cn/>) is a web server with
91 customizable features; Tumor and normal samples in the GEPIA database[17] were derived
92 from The Cancer Genome Atlas (TCGA) and Genotype Tissue Expression (GTEx) programs.
93 GEPIA was used to analyze the overall survival levels and expression levels in disease-free
94 survival. Oncomine (<https://www.oncomine.org/>)[18] was used to analyze DEG expression in

95 hepatic cancer tissues and non-hepatocarcinoma tissues, as well as AURKA and CDKN3
96 expression, tumor grade, hepatitis virus infection status, satellite and vascular invasion
97 relationships.

98 2 results

99 2.1 Article ideas and structure

100 **2.2 DEG screening results** The GSE121248, GSE76427, and GSE60502 datasets were
101 screened out from the GEO database, 1153, 554, 1728 DEGs was found respectively. Finally,
102 an online Venn Diagram tool yielded 215 co-expression DEGs containing 34 common
103 upregulated genes and 181 downregulated genes from the three datasets. (Tab. S1-3, Fig. 2).

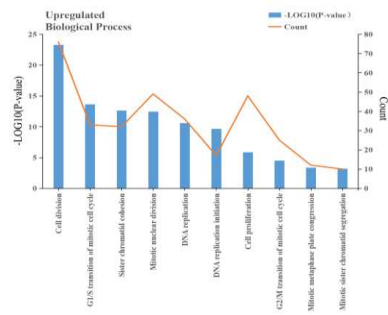


104

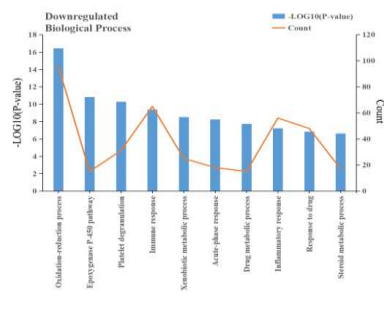
105 **Fig. 2** 215 DEG obtained from the three datasets. **(a)** 34 common upregulated genes. **(b)** 181 common
106 downregulated genes. The different colors represent different datasets, and each intersecting area
107 represents a gene shared between datasets. DEGs with $|\log_{2}FC|$ (fold change) >1 and $\text{adj.}p\text{-value} < 0.05$
108 were selected.

109 **2.3 Analysis of GO enrichment results** The upregulated genes and downregulated genes
110 were input separately into the DAVID Database for GO and KEGG functional enrichment
111 analysis. GO analysis revealed the BP, CC and MF of the first ten upregulated and

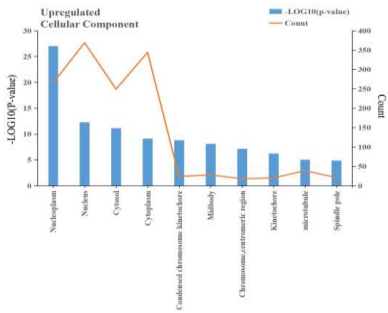
112 downregulated genes (Fig. 3, Tab. S4). The biological processes that were significantly
113 enriched by upregulated genes include cell division, mitotic nuclear division and cell
114 proliferation. In terms of cellular components, the upregulated genes reside mainly in the
115 nucleus, cytoplasm and nucleoplasm. The molecular functions that were most heavily
116 involved were protein binding and ATP binding. For downregulated genes, the biological
117 processes most commonly affected were the oxidation-reduction process and immune
118 response, while heme binding and oxidoreductase activity were the main molecular functions
119 implicated. Downregulated genes were commonly found in the extracellular region and
120 extracellular exosome.



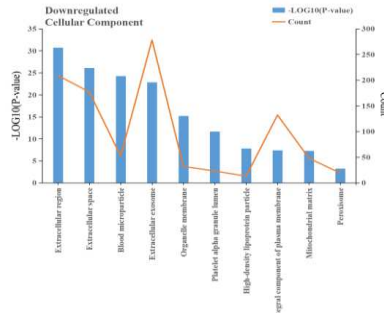
A



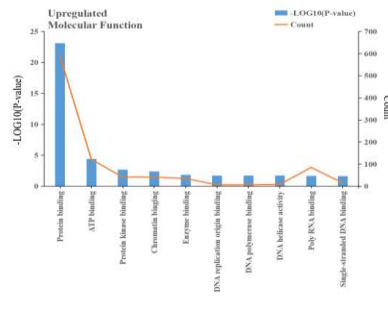
D



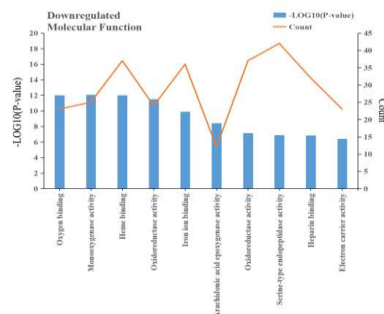
B



E



C

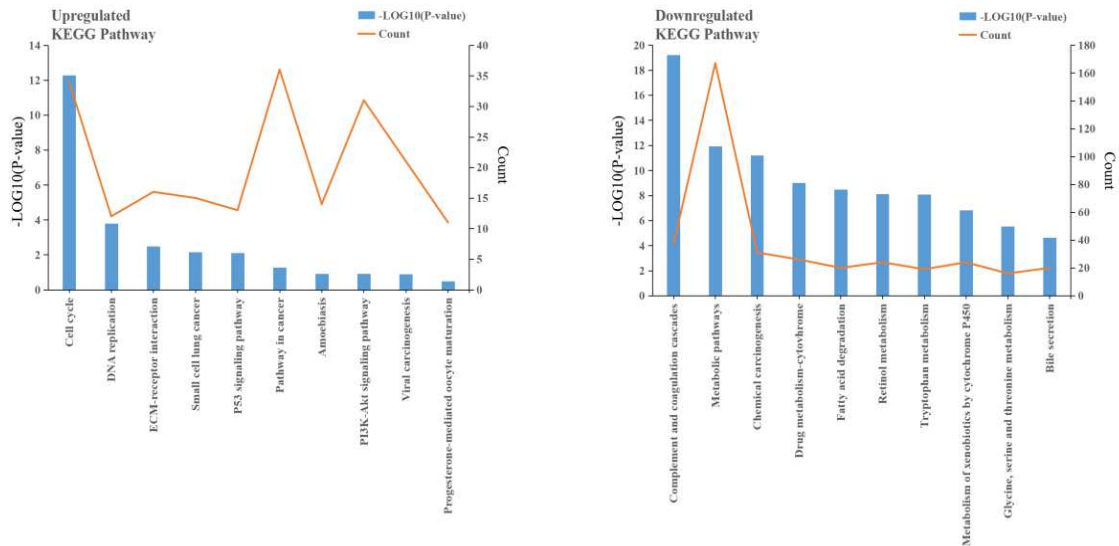


F

121

122 **Fig. 3** Results of GO enrichment analysis of differential genes. GO=Gene ontology. The X-axis refers to the
 123 function of gene, the left-sided Y-axis represents the p-value (-log10), and the right-sided Y-axis represents
 124 the number of genes enriched. Figures A, B, and C represent the GO enrichment results of upregulated
 125 genes; Figures D, E, and F represent the GO enrichment results of downregulated genes.

126 **2.4 Analysis of KEGG enrichment results** Using KEGG, the pathways of the first ten
 127 upregulated and downregulated genes were mapped out (Fig. 4, Tab. S5). Upregulated genes
 128 have been shown to affect the cell cycle and DNA replication while downregulated genes
 129 affected metabolic pathways and chemical carcinogenesis.



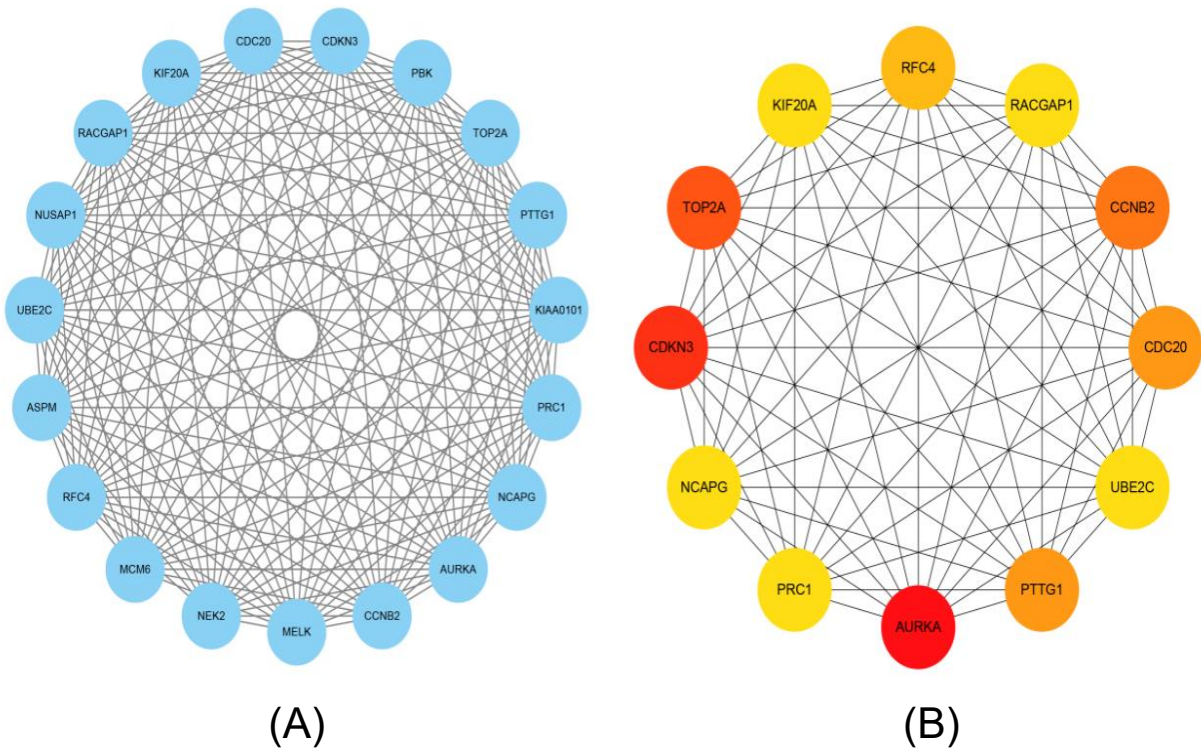
A

B

130

131 **Fig. 4** Results of KEGG enrichment analysis of differential genes. KEGG=Kyoto encyclopedia of genes and
 132 genomes. The X-axis refers to the function of the gene, the left-sided Y-axis represents p-value (-log10),
 133 and the right-sided Y-axis represents the number of enriched genes. Figure A represents the KEGG
 134 enrichment result of upregulated genes; Figure B represents the KEGG enrichment result of
 135 downregulated genes.

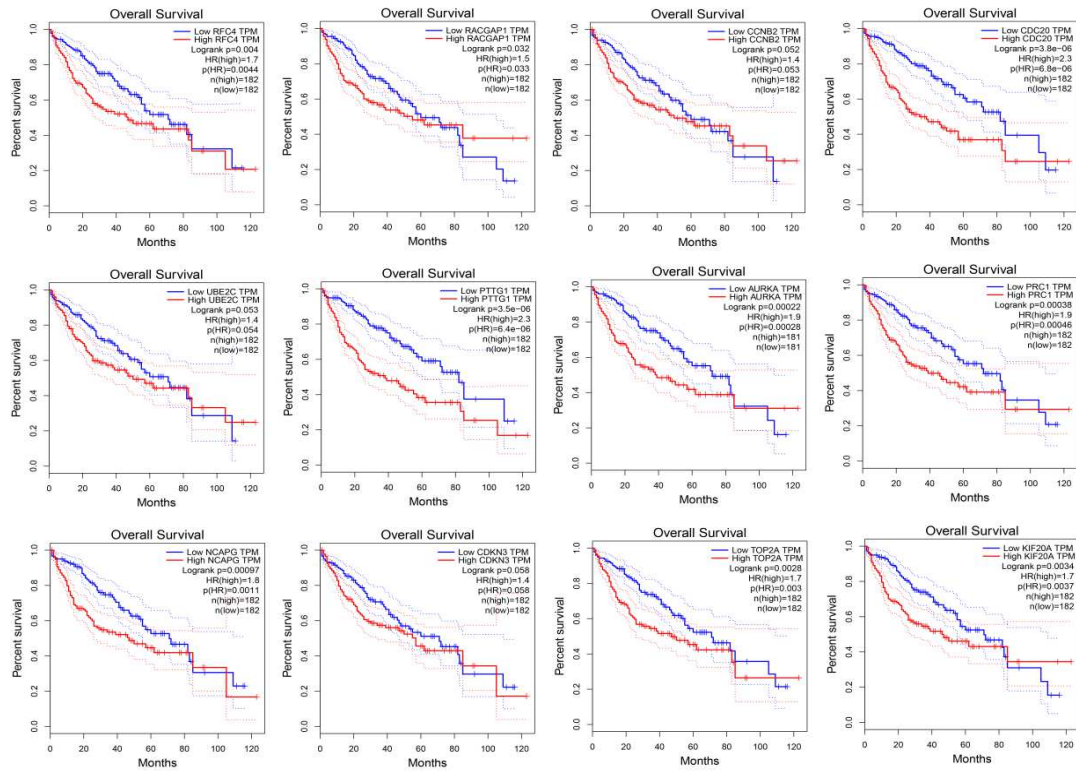
136 **2.5 Screening results of Hub genes** DEGs were imported into the String database. Homo
 137 sapiens analysis was selected and the interaction score was set to 0.4 to obtain a
 138 protein-protein interaction network (Fig. S1). Using Cytoscape software with MCODE and
 139 cytoHubba plugin, the most critical groups in the PPI network were screened out (Fig. 5A),
 140 and top 12 key genes were filtered: AURKA> CDKN3> TOP2A> CCNB2> CDC20 >
 141 PTTG1> RFC4> UBE2C>RACGAP1> KIF20A> NCAPG> PRC1 (Fig. 5B). According to
 142 the MCC algorithm, AURKA and CDKN3 were the two most critical genes. The names,
 143 abbreviations and functions of these central genes are shown in Tab S6.



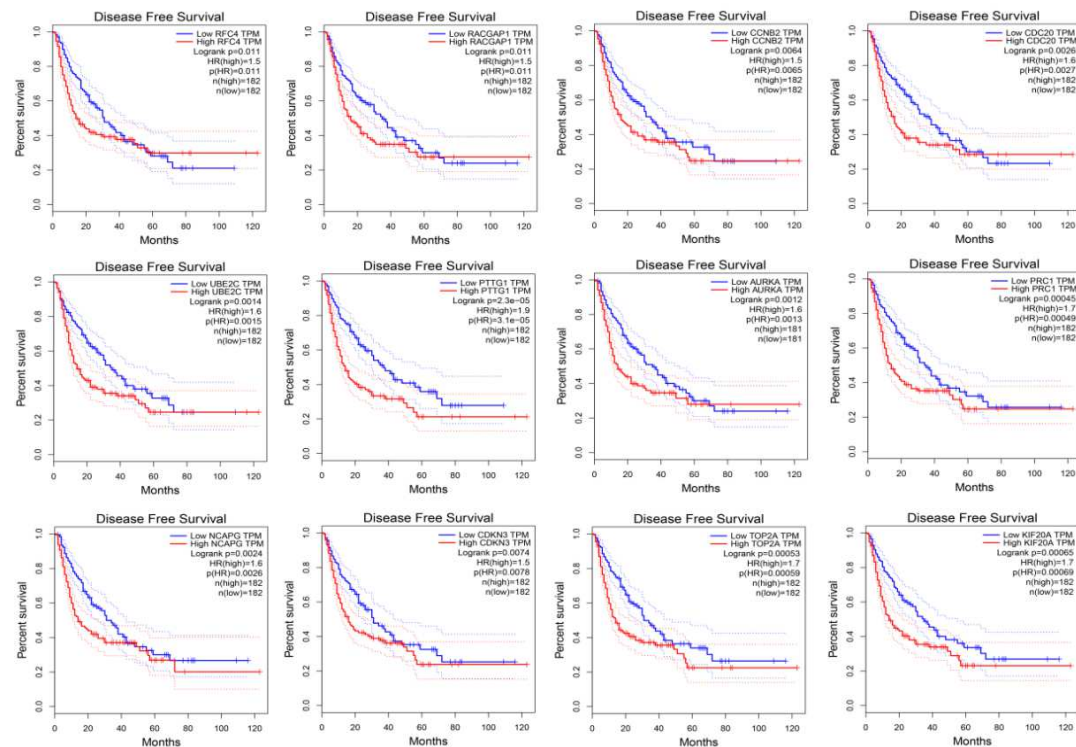
144
145

146 **Fig. 5** MCODE and CytoHubba visualization network. **(A)** The first score gene clusters was screened by
 147 Cytoscape's MCODE plugins. All the genes were upregulated genes, with a network of 19 nodes and 170
 148 edges. **(B)** Using the MCC algorithm of Cytoscape's CytoHubba plugin, the top 12 Hub genes were selected.
 149 All the genes were upregulated genes and the Hub gene network had 12 nodes and 60 edges. The red oval
 150 represents a DEG with high PPI score. The darker the red colour, the higher the PPI score. The edge
 151 represents protein-protein association. Among them, AURKA and CDKN3 were the two highest-scoring
 152 genes.

153 **2.6 Functional analysis of Hub gene** Kaplan-Meier curve was used to analyze the overall
 154 survival and disease-free survival of the central gene. The expression of AURKA, CDC20,
 155 RFC4, KIF20A, RACGAP1, TOP2A, PTTG1, PRC1, NCAPG in HCC patients showed poor
 156 overall survival, $p < 0.05$, while CCNB2, UBE2C, CDKN3 expression in patients was not
 157 significant in overall survival analysis, $p > 0.05$. Nonetheless, HCC patients with AURKA,
 158 CDC20, RFC4, KIF20A, CDKN3, RACGAP1, TOP2A, CCNB2, UBE2C, PTTG1, PRC1,
 159 NCAPG changes showed poorer disease-free survival, $p < 0.05$ (Fig. 6A and B).



A



B

160

161

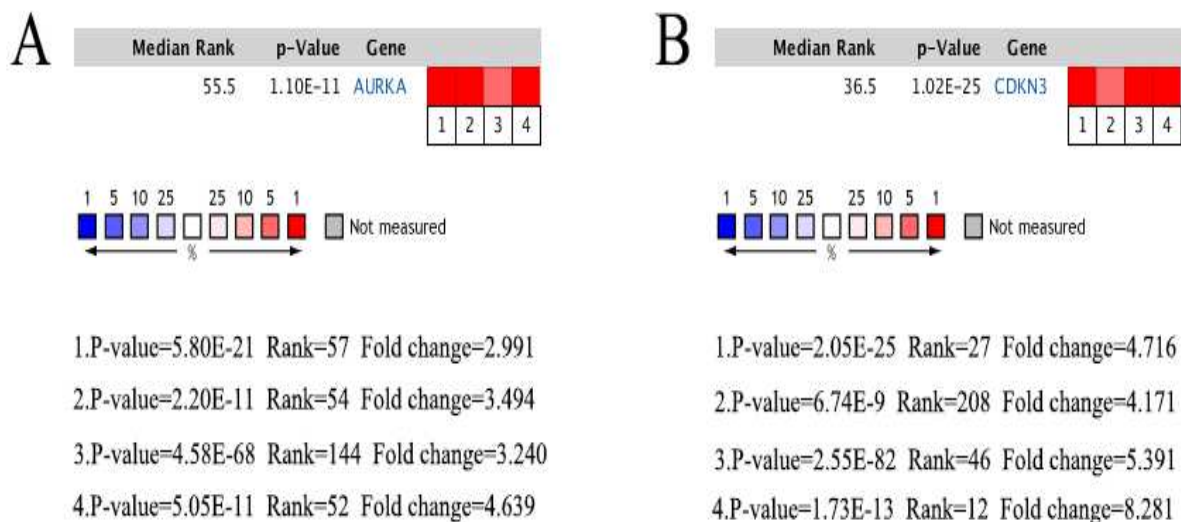
162

163 **Fig. 6** (A) Using the GEPIA online platform for overall survival analysis, patients' AURKA, CDC20, RFC4,
 164 KIF20A, RACGAP1, TOP2A, PTTG1, PRC1 and NCAPG expression were significantly different, while patients'
 165 CCNB2, UBE2C and CDKN3 expression were not significant in the overall survival analysis. The difference of
 166 $p < 0.05$ was considered statistically significant. (B) Using the GEPIA online platform for Disease Free

167 Survival analysis, patients' AURKA, CDC20, RFC4, KIF20A, CDKN3, RACGAP1, TOP2A, CCNB2, UBE2C, PTTG1,
 168 PRC1, and NCAPG were significantly differently expressed, and the difference of $p < 0.05$ was considered
 169 statistically significant. significance.

170 2.7 AURKA and CDKN3 Functional Analysis

171 Among these genes, AURKA and CDKN3 were the two most critical genes in the PPI
 172 network, suggesting that they may play an important role in the development or progression
 173 of HCC. Based on data from GEPIA online platform, we noted that HCC patients with
 174 genomic alterations in AURKA and CDKN3 showed reduced overall and disease-free survival,
 175 as shown in Fig.7 and Fig.8, AURKA (total survival $P = 0.00022$, disease-free survival $P =$
 176 0.0012), CDKN3 (total survival $P = 0.058$, disease-free survival $P = 0.0074$). Oncomine
 177 analysis of cancer vs. normal tissue showed that AURKA and CDKN3 were significantly
 178 overexpressed in HCC in the different datasets (Fig. 7A and B).



179
 180 **Fig. 7** Oncomine analysis of **(A)** AURKA and **(B)** CDKN3 in hepatic cancer tissues and normal tissues. Heat
 181 map of AURKA and CDKN3 gene expression in hepatocellular carcinoma clinical samples and normal
 182 tissues.1. Hepatocellular Carcinoma vs. Normal Chen Liver, Mol Biol Cell, 2002; 2. Hepatocellular
 183 Carcinoma vs. Normal Roessler Liver, Cancer Res, 2010; 3. Hepatocellular Carcinoma vs. Normal Roessler
 184 Liver 2, Cancer Res, 2010;4. Hepatocellular Carcinoma vs. Normal Wurmbach Liver, Hepatology, 2007.

186 **Discussion**

187 In this study, three datasets were selected from the GEO database, which included HCC
188 tissue samples and non-HCC tissue samples. Following the GEO2R analysis of differential
189 genes, 215 DEG were identified, including 34 upregulated genes and 181 downregulated
190 genes. GO enrichment and KEGG functional analysis were performed on these genes.
191 Upregulated genes mainly affected cell division, nucleus, protein binding, and pathway in
192 cancer. Downregulated genes were mainly involved in the oxidation-reduction process,
193 extracellular region, serine-type endopeptidase activity, and metabolic pathways. Besides, a
194 PPI network for the DEG was constructed, and the 12 Hub genes in the differential expression
195 interaction network, including AURKA, CDC20, RFC4, KIF20A, CDKN3, RACGAP1,
196 TOP2A, CCNB2, UBE2C, PTTG1, PRC1 and NCAPG, were screened by the MCODE and
197 MCC algorithm in CytoHubba. Among them, AURKA and CDKN3 were identified as the
198 most important genes.

199 TOP2A is one of the nuclear matrix components. It has been found that overexpression of
200 TOP2A is closely related to breast cancer, prostate cancer and liver cancer[19, 20]. In normal
201 tissues, PTTG1 is expressed in low amounts or not at all in normal tissue. But in malignant
202 tumors such as adrenocortical carcinoma, prostate cancer and oral squamous cell carcinoma,
203 PTTG1 is abnormally highly expressed and plays a role in tumor cell proliferation[21, 22].
204 CCNB2 is highly expressed in various malignant tumors such as lung cancer, breast cancer
205 and gastric cancer, and is significantly associated with poor clinical outcomes and
206 prognosis[23, 24]. PRC1 is phosphorylated by CDK1/CyclinB1 protein kinase during cell
207 mitosis and controls the formation of its multimers by regulating its phosphorylation and

208 dephosphorylation, which in turn affects the formation of the central region of the mitotic
209 spindle[25]. The study found that that PRC1 promotes the early recurrence of hepatocellular
210 carcinoma through the wnt/ β -catenin signaling pathway[26]. UBE2C is involved in the
211 regulation of cell mitosis by mediating the ubiquitination of a ubiquitin ligase E3 - APC/C,
212 which plays an important role in regulating cell cycle progression[27]. KIF20A is a member
213 of the kinesin superfamily and is involved in cell mitosis. In recent years, it has been found
214 that KIF20A is abnormally expressed in some tumor cells and tissues, and its abnormal
215 expression is closely related to the formation and development of tumors[28, 29]. RACGAP1
216 has also been shown to be overexpressed in malignant tumor tissues such as hepatocellular
217 carcinoma, breast cancer and meningioma. Overexpression of RACGAP1 can be used as a
218 marker to evaluate the invasiveness of tumors [30, 31]. NuSAP1 is a microtubule protein that
219 plays an important role in spindle assembly and is an important regulatory molecule in the
220 normal cell cycle. The mRNA and protein levels of NuSAP1 are tightly regulated and exhibit
221 cyclical changes during cell cycle progression[32]. RFC4 is abnormally regulated in various
222 cancers. In a variety of tumors such as colon cancer, breast cancer and liver cancer, silencing
223 RFC4 blocks cells in the S phase, preventing them from subsequent mitosis and proliferation,
224 therefore resulting in a decrease in tumor cell proliferation[33-35]. CDC20 acts as a cell cycle
225 regulator and also plays an important role in human tumors. In numerous tumor types, high
226 expression of CDC20 was observed and this was associated with poor prognosis especially in
227 lung cancer, bladder cancer and liver cancer[36, 37]. NCAPG is a cell cycle-associated gene
228 that affects primary hepatoma cells by influencing mitosis[38].

229

230 AURKA is overexpressed in a variety of human cancers, including gastric cancer,
231 breast cancer, bladder cancer, head and neck squamous cell carcinoma and HCC[39-41]. And
232 it plays an important role in the mitotic cell cycle by participating in centrosome replication,
233 isolation and maturation[42-44]. It was demonstrated that the overexpression or inhibition of
234 AURKA significantly opposed or promoted the anticancer effects of cinobufagin in Huh-7
235 cells, respectively[45]. Genetic variations in the gene encoding AURKA may be a significant
236 predictor of early HCC occurrence and a reliable biomarker for disease progression[46].
237 Additionally, study results suggested that AURKA contributed to metastasis of irradiated
238 residual HCC through facilitating epithelial-mesenchymal transition (EMT) and cancer stem
239 cell (CSC) properties, suggesting the potential clinical application of AURKA inhibitors in
240 radiotherapy for patients with HCC[47]. The study showed that Aurora-A protein is
241 upregulated in HCC tissues and significantly correlated with recurrence-free and overall
242 survival of patients.

243 CDKN3 is a cell cycle regulatory protein that interacts directly or indirectly with
244 Cyclin-dependent protein kinase (CDK) and cyclin-dependent kinase inhibitors [48, 49].
245 CDKN3 exerts different functions in different tumor types. For example, it inhibits cell
246 proliferation in glioblastoma, chronic myeloid leukemia and neuroblastoma[50-52]. It is also a
247 tumor suppressor gene, whereby high expression in liver cancer, lung cancer, ovarian cancer,
248 cervical cancer, kidney cancer, prostate cancer, and breast cancer promotes cell proliferation
249 and facilitates the development of cancer[53-56]. CDKN3 expression may reduce the survival
250 of tumor cells and alter the sensitivity to therapeutic agents via the AKT/P53/P21 signaling
251 pathway. Therefore, CDKN3 may be involved in tumor differentiation and self-renewal[57].

252 In the PPI network, AURKA and CDKN3 are directly linked to genes such as TOP2A
253 and PTTG1, suggesting its important role in HCC. We evaluated the expression of AURKA
254 and CDKN3 in terms of overall and disease-free survival through GEPIA and Oncomine
255 software, which was reduced when there were genetic alterations in AURKA and CDKN3.
256 Although the overall survival analysis of CDKN3 was not statistically significant in this study,
257 some clinical studies have shown that overexpression of CDKN3 is significantly associated
258 with reduced survival times[58]. It had been reported that the overexpression of CDKN3 also
259 had a significant effect on the overall survival of HCC patients[59]. We speculate that this
260 may be because the survival analysis of the GEPIA tool was based on the relationship
261 between gene mutation and prognosis, but gene overexpression is usually caused by mutation
262 or amplification. Besides, the data included in each database is inconsistent and there will be
263 deviations. Therefore, overexpression of CDKN3 in HCC may come from gene amplification
264 rather than mutation, and further research is needed to confirm our hypothesis.

265 In summary, this study was designed to identify DEGs that may be involved in the
266 pathogenesis or progression of HCC. A total of 215 DEGs and 12 Hub genes were identified
267 and can be considered diagnostic biomarkers for HCC. However, further research is needed to
268 elucidate the biological functions of these genes in HCC.

269 **Authors' contributions**

270 Shengshan Wang, Yuning Lin, and Wanjun Chen for acquisition of data, analysis and
271 interpretation of data, statistical analysis and drafting of the manuscript; Delun Huang, Yanfei
272 Wei and Qi Zhang for study concept and design, analysis and interpretation of data, obtained

273 funding. All authors read and approved the final manuscript.

274 **Availability of data and material**

275 The data showed in this article are included in published articles or available from the
276 corresponding author on reasonable request.

277 **Funding**

278 The authors gratefully acknowledge financial support by the National Natural Science
279 Foundation of China (No. 81760757, 81560690), Guangxi Natural Science Foundation Major
280 Project (No. 2017GXNSFAA198152), youth innovation team of Guangxi University of
281 traditional Chinese medicine (2015QT001), Foundation for Guangxi Youth basic ability
282 improving (2020KY07028).

283 **Ethics declarations**

284 **Ethics approval and consent to participate**

285 Not applicable.

286 **Consent for Publication**

287 Not applicable.

288 **Competing interests**

289 The authors declare no financial or another competing interest.

290 **Acknowledgements**

291 The authors would like to thank the staff members in physiology department for their work

292 and support in our scientific work.

293 **References**

- 294 1. Ferlay, J., et al., Cancer incidence and mortality worldwide: sources, methods and major patterns in
295 GLOBOCAN 2012. *Int J Cancer*, 2015. **136**(5): p. E359-86DOI: 10.1002/ijc.29210.
- 296 2. Forner, A., J.M. Llovet, and J. Bruix, Hepatocellular carcinoma. *Lancet*, 2012. **379**(9822): p. 1245-55DOI:
297 10.1016/S0140-6736(11)61347-0.
- 298 3. Ringelhan, M., J.A. McKeating, and U. Protzer, Viral hepatitis and liver cancer. *Philos Trans R Soc Lond B*
299 *Biol Sci*, 2017. **372**(1732)DOI: 10.1098/rstb.2016.0274.
- 300 4. Lohitesh, K., R. Chowdhury, and S. Mukherjee, Resistance a major hindrance to chemotherapy in
301 hepatocellular carcinoma: an insight. *Cancer Cell Int*, 2018. **18**: p. 44DOI: 10.1186/s12935-018-0538-7.
- 302 5. Edgar, R., M. Domrachev, and A.E. Lash, Gene Expression Omnibus: NCBI gene expression and
303 hybridization array data repository. *Nucleic Acids Res*, 2002. **30**(1): p. 207-10DOI:
304 10.1093/nar/30.1.207.
- 305 6. Wang, S.M., L.L. Ooi, and K.M. Hui, Identification and validation of a novel gene signature associated
306 with the recurrence of human hepatocellular carcinoma. *Clin Cancer Res*, 2007. **13**(21): p. 6275-83DOI:
307 10.1158/1078-0432.CCR-06-2236.
- 308 7. Grinchuk, O.V., et al., Tumor-adjacent tissue co-expression profile analysis reveals pro-oncogenic
309 ribosomal gene signature for prognosis of resectable hepatocellular carcinoma. *Mol Oncol*, 2018. **12**(1):
310 p. 89-113DOI: 10.1002/1878-0261.12153.
- 311 8. Wang, Y.H., et al., Plasmalemmal Vesicle Associated Protein (PLVAP) as a therapeutic target for
312 treatment of hepatocellular carcinoma. *BMC Cancer*, 2014. **14**: p. 815DOI: 10.1186/1471-2407-14-815.
- 313 9. Fugelli, P., [General medicine in the 1990's]. *Tidsskr Nor Laegeforen*, 1990. **110**(17): p. 2268-72.
- 314 10. Sanger, D.J. and B. Zivkovic, Discriminative stimulus properties of chlordiazepoxide and zolpidem.
315 Agonist and antagonist effects of CGS 9896 and ZK 91296. *Neuropharmacology*, 1987. **26**(5): p.
316 499-505.
- 317 11. Kanehisa, M., The KEGG database. *Novartis Found Symp*, 2002. **247**: p. 91-101; discussion 101-3,
318 119-28, 244-52.
- 319 12. Horne, L., Nutrition and dietetics in the West Indies. *Hum Nutr Appl Nutr*, 1986. **40**(4): p. 243-52.
- 320 13. Shannon, P., et al., Cytoscape: a software environment for integrated models of biomolecular
321 interaction networks. *Genome Res*, 2003. **13**(11): p. 2498-504DOI: 10.1101/gr.1239303.
- 322 14. Bader, G.D. and C.W. Hogue, An automated method for finding molecular complexes in large protein
323 interaction networks. *BMC Bioinformatics*, 2003. **4**: p. 2.
- 324 15. Chin, C.H., et al., cytoHubba: identifying hub objects and sub-networks from complex interactome.
325 *BMC Syst Biol*, 2014. **8 Suppl 4**: p. S11DOI: 10.1186/1752-0509-8-S4-S11.
- 326 16. Sauer, G. and D. Scholz, [On the purification and characterization of 2,3-PGase of red blood cells]. *Folia*
327 *Haematol Int Mag Klin Morphol Blutforsch*, 1965. **83**(4): p. 377-82.
- 328 17. Seki, M., [Effect of histamine on the kinetics of transfused lymphocytes]. *Saishin Igaku*, 1971. **26**(8): p.
329 1495-501.
- 330 18. Foote, S.L., et al., Electrophysiological evidence for the involvement of the locus coeruleus in alerting,
331 orienting, and attending. *Prog Brain Res*, 1991. **88**: p. 521-32.
- 332 19. Liu, T., et al., Mutual regulation of MDM4 and TOP2A in cancer cell proliferation. *Mol Oncol*, 2019.

- 333 13(5): p. 1047-1058DOI: 10.1002/1878-0261.12457.
- 334 20. Hao, W., L. Zheng, and P. Xin-xing, Curcumol promotes the apoptosis of hepatocellular carcinoma
335 HepG2 cells by regulating PI3K/AKT pathway. *Central South Pharmacy*, 2019. **17**(01): p. 11-14.
- 336 21. Demeure, M.J., et al., PTTG1 overexpression in adrenocortical cancer is associated with poor survival
337 and represents a potential therapeutic target. *Surgery*, 2013. **154**(6): p. 1405-16; discussion 1416DOI:
338 10.1016/j.surg.2013.06.058.
- 339 22. Cao, X.L., et al., [Downregulation of PTTG1 expression inhibits the proliferation and invasiveness and
340 promotes the apoptosis of human prostate cancer LNCaP-AI cells]. *Zhonghua Nan Ke Xue*, 2017. **23**(7):
341 p. 589-597.
- 342 23. Albulescu, R., Elevated cyclin B2 expression in invasive breast carcinoma is associated with unfavorable
343 clinical outcome. *Biomark Med*, 2013. **7**(2): p. 203.
- 344 24. Shi, Q., et al., ISL1, a novel regulator of CCNB1, CCNB2 and c-MYC genes, promotes gastric cancer cell
345 proliferation and tumor growth. *Oncotarget*, 2016. **7**(24): p. 36489-36500DOI:
346 10.18632/oncotarget.9269.
- 347 25. Hoffmann, I.M., et al., Acute renal failure in cystic fibrosis: association with inhaled tobramycin therapy.
348 *Pediatr Pulmonol*, 2002. **34**(5): p. 375-7DOI: 10.1002/ppul.10185.
- 349 26. Chen, J., et al., The microtubule-associated protein PRC1 promotes early recurrence of hepatocellular
350 carcinoma in association with the Wnt/beta-catenin signalling pathway. *Gut*, 2016. **65**(9): p.
351 1522-34DOI: 10.1136/gutjnl-2015-310625.
- 352 27. Han, Q., et al., MicroRNA-196a post-transcriptionally upregulates the UBE2C proto-oncogene and
353 promotes cell proliferation in breast cancer. *Oncol Rep*, 2015. **34**(2): p. 877-83DOI:
354 10.3892/or.2015.4049.
- 355 28. Stangel, D., et al., Kif20a inhibition reduces migration and invasion of pancreatic cancer cells. *J Surg Res*,
356 2015. **197**(1): p. 91-100DOI: 10.1016/j.jss.2015.03.070.
- 357 29. Lu, M., et al., Aberrant KIF20A expression might independently predict poor overall survival and
358 recurrence-free survival of hepatocellular carcinoma. *IUBMB Life*, 2018. **70**(4): p. 328-335DOI:
359 10.1002/iub.1726.
- 360 30. Neubauer, E., et al., Comparative evaluation of three proliferation markers, Ki-67, TOP2A, and RacGAP1,
361 in bronchopulmonary neuroendocrine neoplasms: Issues and prospects. *Oncotarget*, 2016. **7**(27): p.
362 41959-41973DOI: 10.18632/oncotarget.9747.
- 363 31. Wang, S.M., L.L. Ooi, and K.M. Hui, Upregulation of Rac GTPase-activating protein 1 is significantly
364 associated with the early recurrence of human hepatocellular carcinoma. *Clin Cancer Res*, 2011. **17**(18):
365 p. 6040-51DOI: 10.1158/1078-0432.CCR-11-0557.
- 366 32. Wang, Y., et al., Downregulation of nucleolar and spindle-associated protein 1 expression suppresses
367 liver cancer cell function. *Exp Ther Med*, 2019. **17**(4): p. 2969-2978DOI: 10.3892/etm.2019.7314.
- 368 33. Wang, X.C., et al., Genome-wide RNAi Screening Identifies RFC4 as a Factor That Mediates
369 Radioresistance in Colorectal Cancer by Facilitating Nonhomologous End Joining Repair. *Clin Cancer Res*,
370 2019DOI: 10.1158/1078-0432.CCR-18-3735.
- 371 34. Chen, Z., et al., Identification of Potential Key Genes for Hepatitis B Virus-Associated Hepatocellular
372 Carcinoma by Bioinformatics Analysis. *J Comput Biol*, 2019. **26**(5): p. 485-494DOI:
373 10.1089/cmb.2018.0244.
- 374 35. Koleck, T.A., et al., An exploratory study of host polymorphisms in genes that clinically characterize
375 breast cancer tumors and pretreatment cognitive performance in breast cancer survivors. *Breast
376 Cancer (Dove Med Press)*, 2017. **9**: p. 95-110DOI: 10.2147/BCTT.S123785.

- 377 36. Kim, Y., et al., MAD2 and CDC20 are upregulated in high-grade squamous intraepithelial lesions and
378 squamous cell carcinomas of the uterine cervix. *Int J Gynecol Pathol*, 2014. **33**(5): p. 517-23DOI:
379 10.1097/PGP.0000000000000082.
- 380 37. Zhuang, L., Z. Yang, and Z. Meng, Upregulation of BUB1B, CCNB1, CDC7, CDC20, and MCM3 in Tumor
381 Tissues Predicted Worse Overall Survival and Disease-Free Survival in Hepatocellular Carcinoma
382 Patients. *Biomed Res Int*, 2018. **2018**: p. 7897346DOI: 10.1155/2018/7897346.
- 383 38. Arai, T., et al., Regulation of NCAPG by miR-99a-3p (passenger strand) inhibits cancer cell
384 aggressiveness and is involved in CRPC. *Cancer Med*, 2018. **7**(5): p. 1988-2002DOI:
385 10.1002/cam4.1455.
- 386 39. Lee, J.W., et al., Combined Aurora Kinase A (AURKA) and WEE1 Inhibition Demonstrates Synergistic
387 Antitumor Effect in Squamous Cell Carcinoma of the Head and Neck. *Clin Cancer Res*, 2019. **25**(11): p.
388 3430-3442DOI: 10.1158/1078-0432.CCR-18-0440.
- 389 40. Guo, M., et al., Increased AURKA promotes cell proliferation and predicts poor prognosis in bladder
390 cancer. *BMC Syst Biol*, 2018. **12**(Suppl 7): p. 118DOI: 10.1186/s12918-018-0634-2.
- 391 41. Wang, L., et al., Gossypin inhibits gastric cancer growth by direct targeting of AURKA and RSK2.
392 *Phytother Res*, 2019. **33**(3): p. 640-650DOI: 10.1002/ptr.6253.
- 393 42. Treekitkarnmongkol, W., et al., Aurora kinase-A overexpression in mouse mammary epithelium induces
394 mammary adenocarcinomas harboring genetic alterations shared with human breast cancer.
395 *Carcinogenesis*, 2016. **37**(12): p. 1180-1189DOI: 10.1093/carcin/bgw097.
- 396 43. Woo, J.K., et al., Daurinol Enhances the Efficacy of Radiotherapy in Lung Cancer via Suppression of
397 Aurora Kinase A/B Expression. *Mol Cancer Ther*, 2015. **14**(7): p. 1693-704DOI:
398 10.1158/1535-7163.MCT-14-0960.
- 399 44. Goos, J.A., et al., Aurora kinase A (AURKA) expression in colorectal cancer liver metastasis is associated
400 with poor prognosis. *Br J Cancer*, 2013. **109**(9): p. 2445-52DOI: 10.1038/bjc.2013.608.
- 401 45. Zhao, L., et al., The anticancer effects of cinobufagin on hepatocellular carcinoma Huh7 cells are
402 associated with activation of the p73 signaling pathway. *Mol Med Rep*, 2019. **19**(5): p. 4119-4128DOI:
403 10.3892/mmr.2019.10108.
- 404 46. Wang, B., et al., Variations in the AURKA Gene: Biomarkers for the Development and Progression of
405 Hepatocellular Carcinoma. *Int J Med Sci*, 2018. **15**(2): p. 170-175DOI: 10.7150/ijms.22513.
- 406 47. Chen, C., et al., AURKA promotes cancer metastasis by regulating epithelial-mesenchymal transition
407 and cancer stem cell properties in hepatocellular carcinoma. *Biochem Biophys Res Commun*, 2017.
408 **486**(2): p. 514-520DOI: 10.1016/j.bbrc.2017.03.075.
- 409 48. Mangini, N.S., et al., Palbociclib: A Novel Cyclin-Dependent Kinase Inhibitor for Hormone
410 Receptor-Positive Advanced Breast Cancer. *Ann Pharmacother*, 2015. **49**(11): p. 1252-60DOI:
411 10.1177/1060028015602273.
- 412 49. Diallo, A. and C. Prigent, [The serine/threonine kinases that control cell cycle progression as
413 therapeutic targets]. *Bull Cancer*, 2011. **98**(11): p. 1335-45DOI: 10.1684/bdc.2011.1467.
- 414 50. Li, H., et al., KAP regulates ROCK2 and Cdk2 in an RNA-activated glioblastoma invasion pathway.
415 *Oncogene*, 2015. **34**(11): p. 1432-41DOI: 10.1038/onc.2014.49.
- 416 51. Poon, R.Y. and T. Hunter, Dephosphorylation of Cdk2 Thr160 by the cyclin-dependent kinase-interacting
417 phosphatase KAP in the absence of cyclin. *Science*, 1995. **270**(5233): p. 90-3DOI:
418 10.1126/science.270.5233.90.
- 419 52. Cress, W.D., P. Yu, and J. Wu, Expression and alternative splicing of the cyclin-dependent kinase
420 inhibitor-3 gene in human cancer. *Int J Biochem Cell Biol*, 2017. **91**(Pt B): p. 98-101DOI:

- 421 10.1016/j.biocel.2017.05.013.
- 422 53. Wang, L., et al., Cyclin-dependent kinase inhibitor 3 (CDKN3) novel cell cycle computational network
423 between human non-malignancy associated hepatitis/cirrhosis and hepatocellular carcinoma (HCC)
424 transformation. *Cell Prolif*, 2011. **44**(3): p. 291-9DOI: 10.1111/j.1365-2184.2011.00752.x.
- 425 54. Fan, C., et al., Overexpression of major CDKN3 transcripts is associated with poor survival in lung
426 adenocarcinoma. *Br J Cancer*, 2015. **113**(12): p. 1735-43DOI: 10.1038/bjc.2015.378.
- 427 55. Li, T., et al., CDKN3 is an independent prognostic factor and promotes ovarian carcinoma cell
428 proliferation in ovarian cancer. *Oncol Rep*, 2014. **31**(4): p. 1825-31DOI: 10.3892/or.2014.3045.
- 429 56. Berumen, J., A.M. Espinosa, and I. Medina, Targeting CDKN3 in cervical cancer. *Expert Opin Ther*
430 *Targets*, 2014. **18**(10): p. 1149-62DOI: 10.1517/14728222.2014.941808.
- 431 57. Dai, W., et al., CDKN3 expression is negatively associated with pathological tumor stage and CDKN3
432 inhibition promotes cell survival in hepatocellular carcinoma. *Mol Med Rep*, 2016. **14**(2): p.
433 1509-14DOI: 10.3892/mmr.2016.5410.
- 434 58. Xing, C., et al., Cyclin-dependent kinase inhibitor 3 is overexpressed in hepatocellular carcinoma and
435 promotes tumor cell proliferation. *Biochem Biophys Res Commun*, 2012. **420**(1): p. 29-35DOI:
436 10.1016/j.bbrc.2012.02.107.
- 437 59. Wu, M., et al., Analysis of potential key genes in very early hepatocellular carcinoma. *World J Surg*
438 *Oncol*, 2019. **17**(1): p. 77DOI: 10.1186/s12957-019-1616-6.

439

Figures

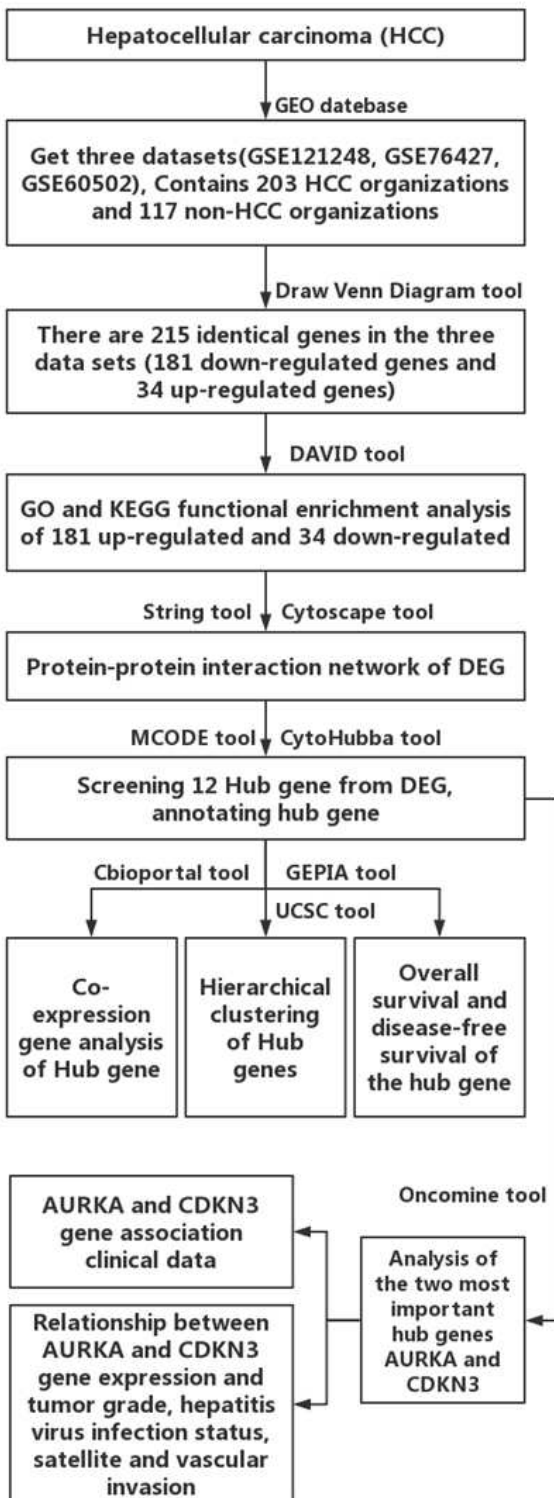


Figure 1

The schematic of this study is intended to describe bioinformatics screening and analysis of key genes for HCC.

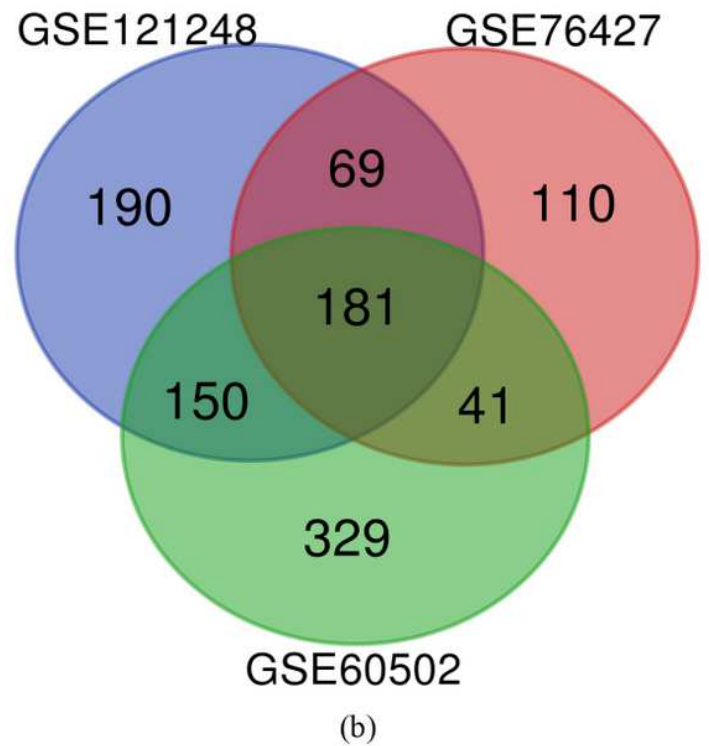
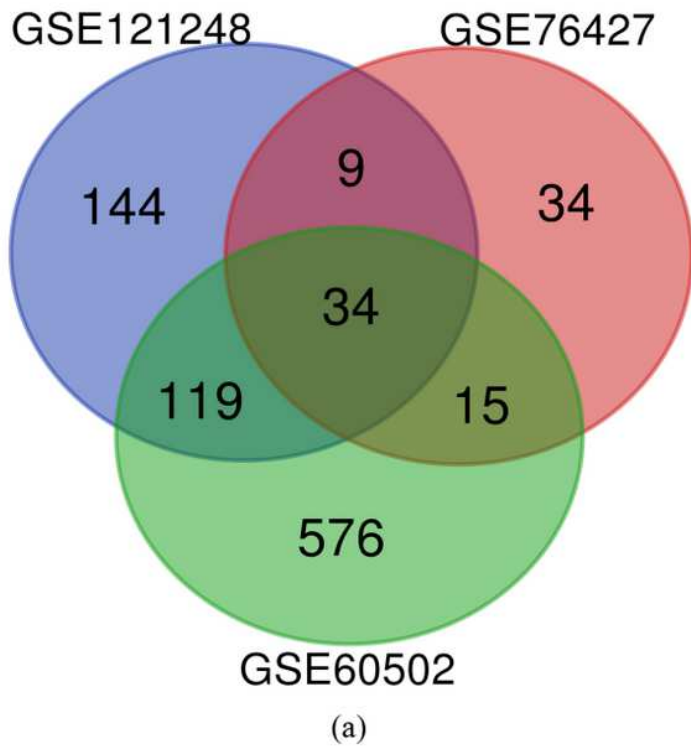
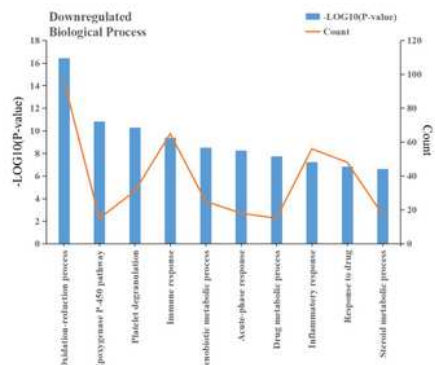
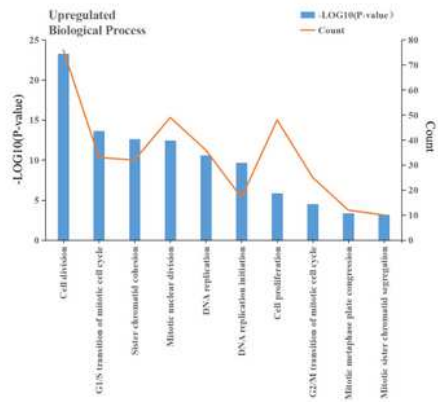


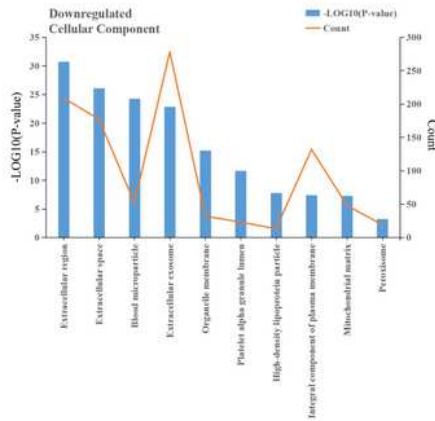
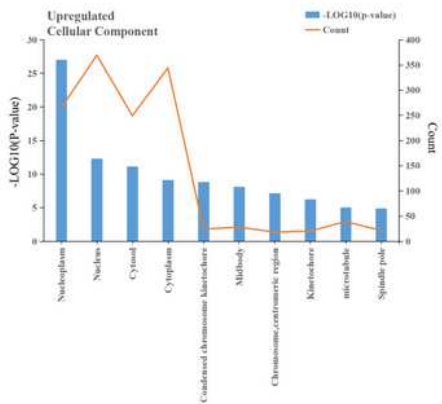
Figure 2

215 DEG obtained from the three datasets. (a) 34 common upregulated genes. (b) 181 common downregulated genes. The different colors represent different datasets, and each intersecting area represents a gene shared between datasets. DEGs with $|\log_{2}FC|$ (fold change) >1 and $\text{adj.p-value} < 0.05$ were selected.



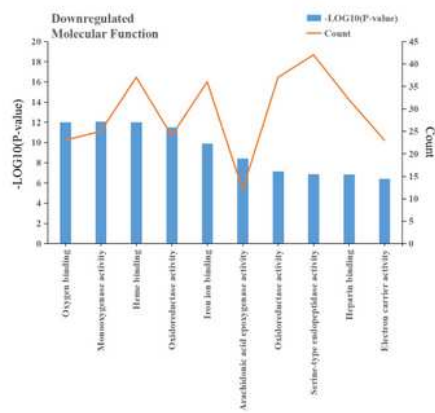
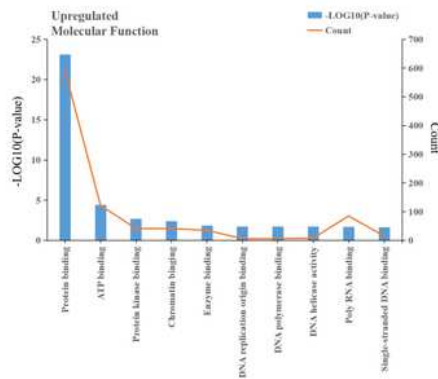
A

D



B

E

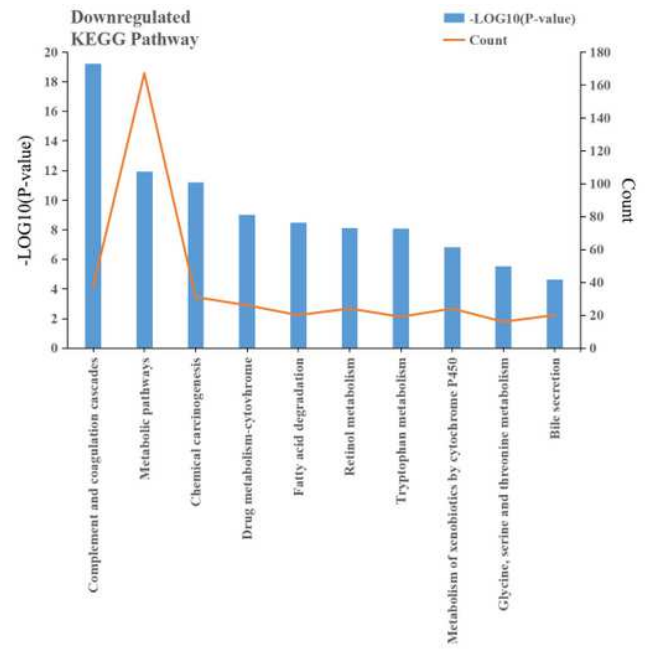
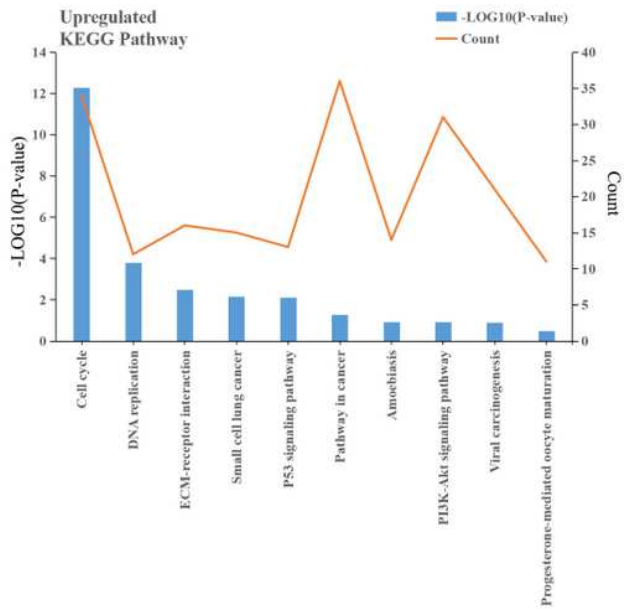


C

F

Figure 3

Results of GO enrichment analysis of differential genes. GO=Gene ontology. The X-axis refers to the function of gene, the left-sided Y-axis represents the p-value (-log10), and the right-sided Y-axis represents the number of genes enriched. Figures A, B, and C represent the GO enrichment results of upregulated genes; Figures D, E, and F represent the GO enrichment results of downregulated genes.



A

B

Figure 4

Results of KEGG enrichment analysis of differential genes. KEGG=Kyoto encyclopedia of genes and genomes. The X-axis refers to the function of the gene, the left-sided Y-axis represents p-value (-log10), and the right-sided Y-axis represents the number of enriched genes. Figure A represents the KEGG enrichment result of upregulated genes; Figure B represents the KEGG enrichment result of downregulated genes.

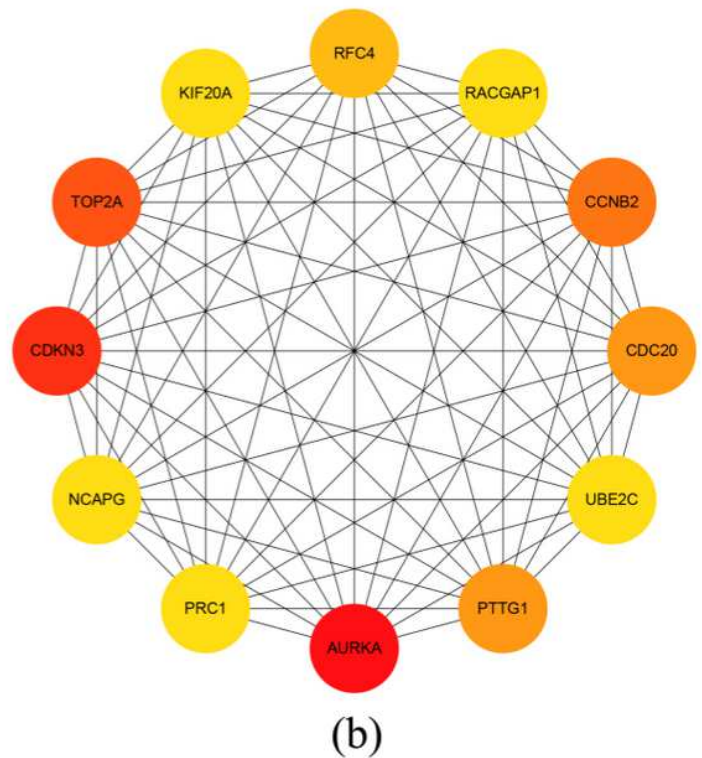
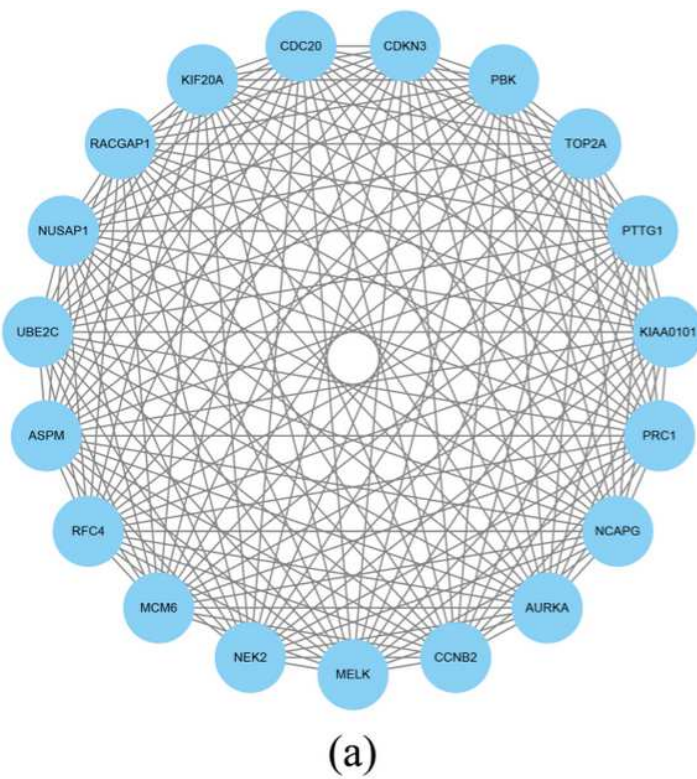


Figure 5

MCODE and CytoHubba visualization network. (A) The first score gene clusters was screened by Cytoscape's MCODE plugins. All the genes were upregulated genes, with a network of 19 nodes and 170 edges. (B) Using the MCC algorithm of Cytoscape's CytoHubba plugin, the top 12 Hub genes were selected. All the genes were upregulated genes and the Hub gene network had 12 nodes and 60 edges. The red oval represents a DEG with high PPI score. The darker the red colour, the higher the PPI score. The edge represents protein-protein association. Among them, AURKA and CDKN3 were the two highest-scoring genes.

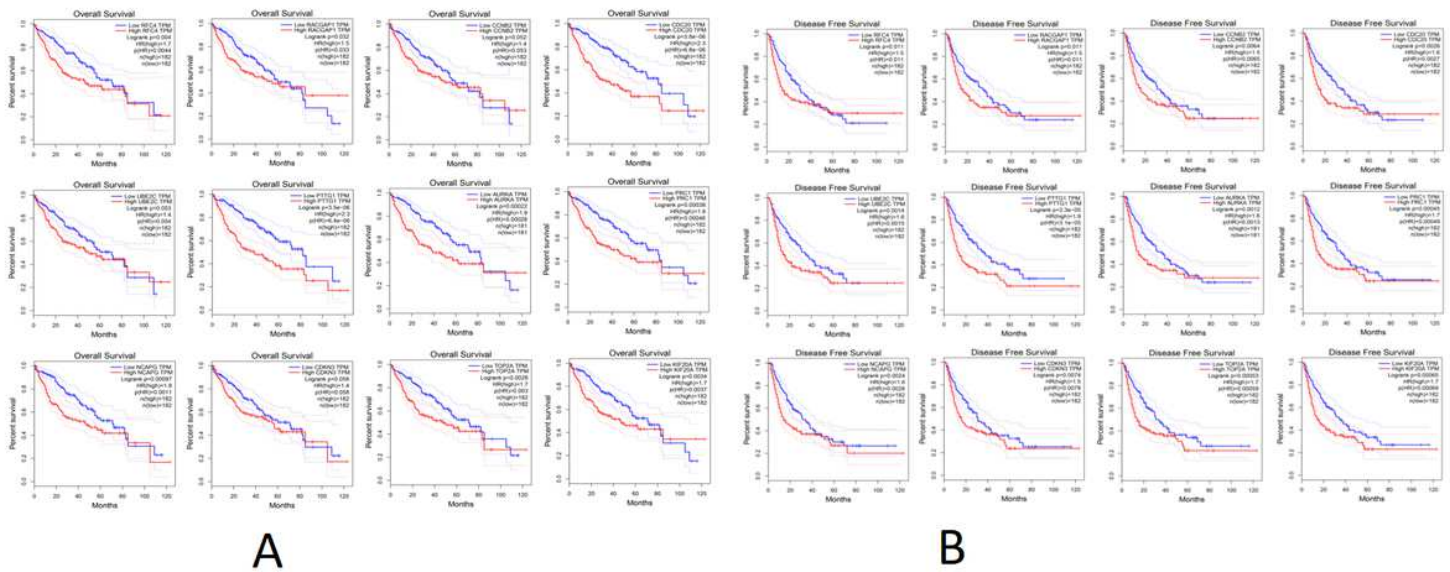
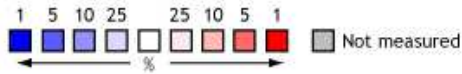
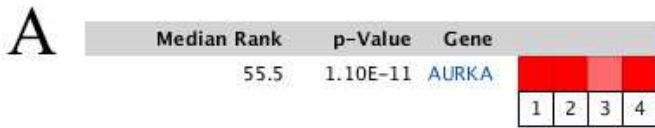
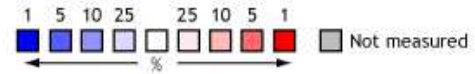
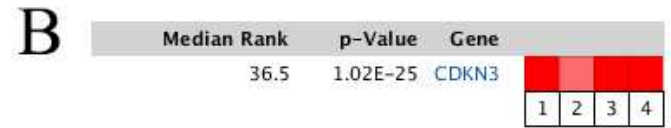


Figure 6

(A) Using the GEPIA online platform for overall survival analysis, patients' AURKA, CDC20, RFC4, KIF20A, RACGAP1, TOP2A, PTTG1, PRC1 and NCAPG expression were significantly different, while patients' CCNB2, UBE2C and CDKN3 expression were not significant in the overall survival analysis. The difference of $p < 0.05$ was considered statistically significant. (B) Using the GEPIA online platform for Disease Free Survival analysis, patients' AURKA, CDC20, RFC4, KIF20A, CDKN3, RACGAP1, TOP2A, CCNB2, UBE2C, PTTG1, PRC1, and NCAPG were significantly differently expressed, and the difference of $p < 0.05$ was considered statistically significant.



1.P-value=5.80E-21 Rank=57 Fold change=2.991
 2.P-value=2.20E-11 Rank=54 Fold change=3.494
 3.P-value=4.58E-68 Rank=144 Fold change=3.240
 4.P-value=5.05E-11 Rank=52 Fold change=4.639



1.P-value=2.05E-25 Rank=27 Fold change=4.716
 2.P-value=6.74E-9 Rank=208 Fold change=4.171
 3.P-value=2.55E-82 Rank=46 Fold change=5.391
 4.P-value=1.73E-13 Rank=12 Fold change=8.281

Figure 7

Oncomine analysis of (A) AURKA and (B) CDKN3 in hepatic cancer tissues and normal tissues. Heat map of AURKA and CDKN3 gene expression in hepatocellular carcinoma clinical samples and normal tissues. 1. Hepatocellular Carcinoma vs. Normal Chen Liver, Mol Biol Cell, 2002; 2. Hepatocellular Carcinoma vs. Normal Roessler Liver, Cancer Res, 2010; 3. Hepatocellular Carcinoma vs. Normal Roessler Liver 2, Cancer Res, 2010; 4. Hepatocellular Carcinoma vs. Normal Wurmbach Liver, Hepatology, 2007.

Supplementary Files

This is a list of supplementary files associated with this preprint. Click to download.

- [Supplementary20200721.docx](#)